

CFD VALIDATION OF STRATIFIED TWO-PHASE FLOWS IN A HORIZONTAL CHANNEL

Christophe Vallée and Thomas Höhne

1. Introduction

In different scenarios of small break Loss of Coolant Accident (SB-LOCA), stratified two-phase flow regimes can occur in the main cooling lines of pressurized water reactors. Because these flow patterns cannot be predicted with the required accuracy and spatial resolution by the one-dimensional system codes, the stratified flows are increasingly modelled with computational fluid dynamics (CFD) codes. In CFD, closure models are required that must be validated, especially if they are to be applied to reactor safety issues.

Slug flow is a challenging flow regime for CFD, because of the acceleration of the gaseous phase and of the transition of the fast liquid slugs, which carry a significant amount of liquid with high kinetic energy. Further, it is potentially hazardous to the structure of the system due to the strong oscillating pressure levels formed behind the liquid slugs as well as the mechanical momentum of the slugs. CFD calculations of slug flow were performed and were compared with optical observations captured at the **Horizontal Air/Water Channel (HAWAC)** of the *Forschungszentrum Dresden-Rossendorf (FZD)*. It is the aim of the conducted simulations to validate the prediction of slug flow with the existing multiphase flow models available in the commercial code *ANSYS CFX* [1]. Further, it is of interest to prove the understanding of the general fluid dynamic mechanism leading to slug flow and to identify the critical parameters affecting the main slug flow parameters (like e.g. slug frequency and propagation velocity).

2. The Horizontal Air/Water Channel (HAWAC)

Experiments were carried out at the **Horizontal Air/Water Channel (Fig. 1)**, which is devoted to co-current flow experiments [2]. The 8 m long test-section has a rectangular cross-section of 100 x 30 mm² (height x width), leading to a length-to-height $L/h = 80$.

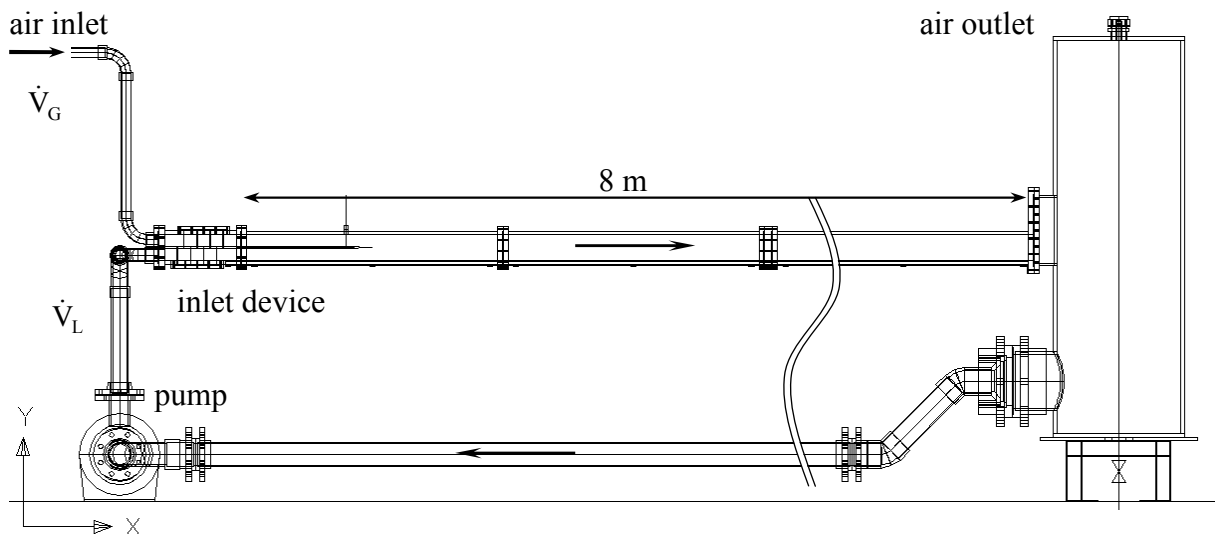


Fig. 1: Schematic view of the horizontal air/water channel (HAWAC)

A special inlet device (Fig. 2) was designed to provide defined boundary conditions at the channel inlet. Therefore, air and water have to be injected separately into the test-section: the air flows through the upper part and the water through the lower part of the inlet device. In order to provide homogenous velocity profiles at the test-section inlet, 4 wire cloth filters are mounted in each part of the inlet device. Air and water come in contact at the edge of a 500 mm long blade that divides both phases downstream of the filter segment. The free inlet cross-section for each phase can be controlled by inclining this blade up and down. In this way, the perturbation caused by the first contact between gas and liquid can be either minimised or, if required, a perturbation can be introduced (e.g. hydraulic jump). Both, filters and the inclinable blade, provide well-defined inlet boundary conditions for the CFD model and therefore offer very good validation possibilities.

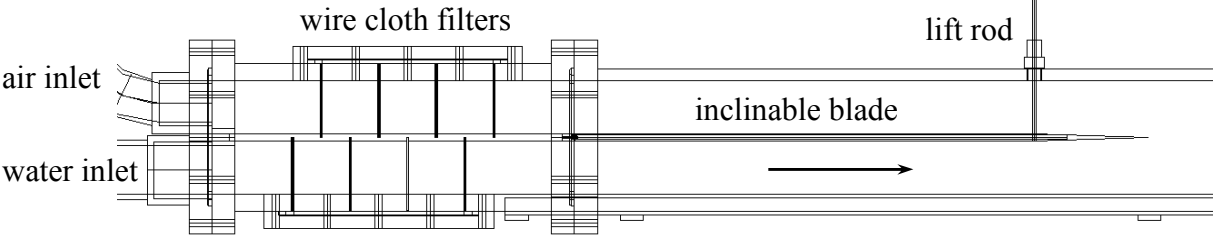


Fig. 2: The inlet device

The maximum superficial velocities achieved in the test-section are 2 m/s for the water and 8 m/s for the air. A flow pattern map (Fig. 3) was established on the basis of visual observations of the flow structure at different combinations of the gas and liquid superficial velocities. The observed flow patterns are: stratified flow, wavy flow, elongated bubble flow and slug flow.

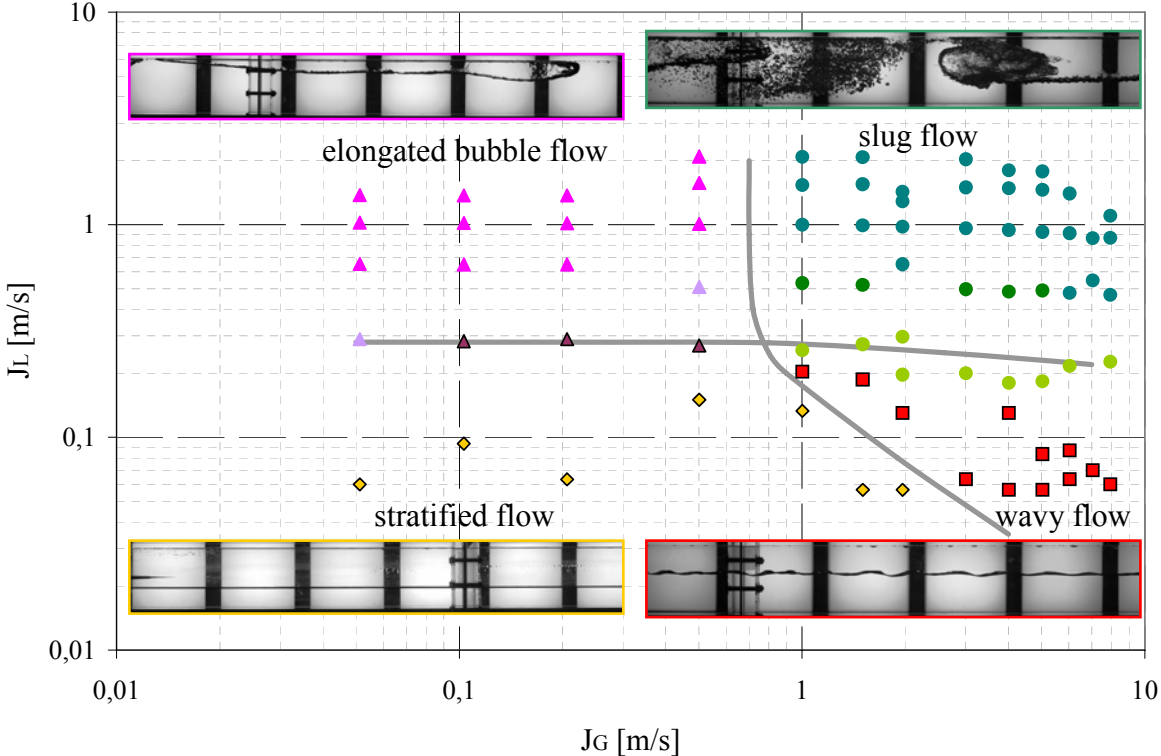


Fig. 3: Flow pattern map for the rectangular channel (inlet blade in horizontal position)

3. CFD model of the channel

The channel with rectangular cross-section was modelled using *ANSYS CFX* [1]. The model dimensions are 4000 x 100 x 30 mm³ (length x height x width), which corresponds to the first half of the test-section. The grid consists of 6 x 10⁵ hexahedral elements.

A slug flow experiment at a superficial water velocity of 1.0 m/s and a superficial air velocity of 5.0 m/s was chosen for the CFD calculations. In the experiment, the inlet blade was in horizontal position. Accordingly, the model inlet was divided into two parts: in the lower 50% of the inlet cross-section, water was injected and in the upper 50% air. An initial water level of $y_0 = 50$ mm was assumed for the entire model length.

In the simulation, both phases have been treated as isothermal and incompressible, at 25°C and at a reference pressure of 1 bar. A hydrostatic pressure was assumed for the liquid phase. Buoyancy effects between the two phases are taken into account by the directed gravity term. At the inlet, the turbulence properties were set using the “Medium intensity and Eddy viscosity ratio” option of the flow solver. This is equivalent to a turbulence intensity of 5% in both phases. The inner surface of the channel walls has been defined as hydraulically smooth with a non-slip boundary condition applied to both gaseous and liquid phases. The channel outlet was modelled with a pressure controlled outlet boundary condition.

As it was the goal of the CFD calculation to induce surface instabilities, which are later generating waves and slugs, the interfacial momentum exchange and also the turbulence parameters had to be modelled correctly. Without any special treatment of the free surface, the high velocity gradients at the free surface, especially in the gaseous phase, generate too high turbulence throughout the two-phase flow when using the differential eddy viscosity models like the k - ϵ or the k - ω model [1]. Therefore, certain damping of turbulence is necessary in the interfacial area because the mesh is too coarse to resolve the velocity gradient in the gas at the interface. On the gas side of the smooth free surface, this damping should be similar to that used near a solid wall. Moreover, on the liquid side the advanced model should take the anisotropy between the normal and the tangential Reynolds stresses into account. Yegorov [2] proposed a simple grid dependent symmetric damping procedure. This procedure provides for the solid wall-like damping of turbulence in both gas and liquid phases. It is based on the standard ω -equation, formulated by Wilcox [1] as follows:

$$\frac{\partial}{\partial t}(\rho \cdot \omega) + \nabla \cdot (\rho \cdot \mathbf{U} \cdot \omega) = \alpha \cdot \frac{\rho \cdot \omega}{k} \cdot \tau_t \cdot \dot{S} - \beta \cdot \rho \cdot \omega^2 + \nabla \cdot [(\mu + \sigma_\omega \cdot \mu_t) \cdot \nabla \omega] \quad (1)$$

where $\alpha = 0.52$ and $\beta = 0.075$ are the k - ω model closure coefficients of the generation and the destruction terms in the ω -equation, $\sigma_\omega = 0.5$ is the inverse of the turbulent Prandtl number for ω , τ_t is the Reynolds stress tensor, and \dot{S} is the strain-rate tensor.

In order to mimic the turbulence damping near the free surface, Yegorov [2] introduced the following source term in the right hand side of the gas and liquid phase ω -equations (1):

$$A \cdot \Delta y \cdot \beta \cdot \rho_i \left(B \cdot \frac{6 \cdot \mu_i}{\beta \cdot \rho_i \cdot \Delta n^2} \right)^2 \quad (2)$$

Here A is the interface area density, Δn is the typical grid cell size across the interface, ρ_i and μ_i are the density and viscosity of the phase i . The factor A activates this source term only at the free surface, where it cancels the standard ω -destruction term of the ω -equation ($-r_i \cdot \beta \cdot \rho_i \cdot \omega_i^2$) and enforces the required high value of ω_i and thus the turbulence damping.

The parallel transient calculation of 5.0 s of simulation time on 4 processors lasts 4 days. A high-resolution discretization scheme was used. For time integration, the fully implicit second order backward Euler method was applied with a constant time step of $dt = 0.001$ s and a maximum of 15 coefficient loops. A convergence in terms of the RMS values of the residuals to be less than 10^{-4} could be assured most of the time.

4. Results

Optical measurements were performed with a high-speed video camera. In the following picture sequences (Fig. 5 and 6), a comparison is presented between CFD calculation and experiment: the calculated phase distribution is visualized and comparable camera frames are shown.

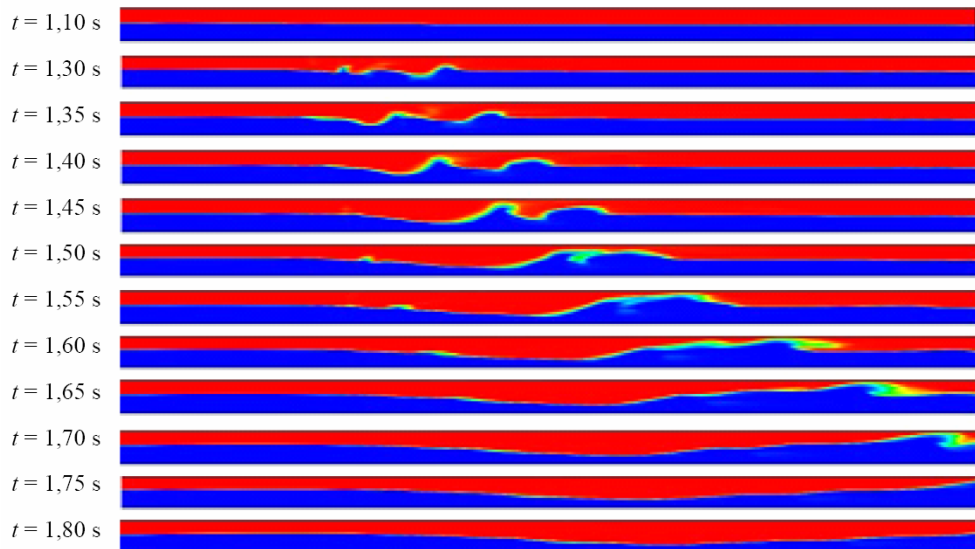


Fig. 5: Calculated sequence of void fraction at $J_L = 1.0$ m/s and $J_G = 5.0$ m/s (depicted part of the channel: 1.4 to 4 m after the inlet)

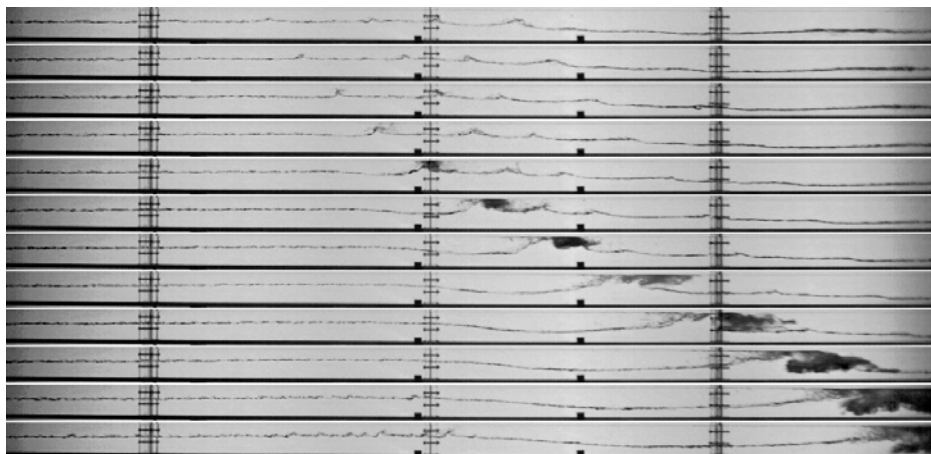


Fig. 6: Measured picture sequence at $J_L = 1.0$ m/s and $J_G = 5.0$ m/s with $\Delta t = 50$ ms (depicted part of the channel: 0 to 3.2 m after the inlet)

In both cases, a slug is generated. The sequences show that the qualitative behaviour of the creation and propagation of the slug is similar in the experiment and in the calculation. In the CFD calculation, the slug develops at approximately $t = 1.30$ s after the beginning of the simulation, induced by instabilities.

The single effects leading to slug flow that can be simulated are shown in details in Fig. 7. These phenomena are:

- Instabilities and small waves are randomly generated by the interfacial momentum transfer (Fig. 7-a). As a result bigger waves are generated.
- The waves can have different velocities and can merge (Fig. 7-b and c).
- Bigger waves roll over (Fig. 7-c) and can close the channel cross-section (Fig. 7-d).

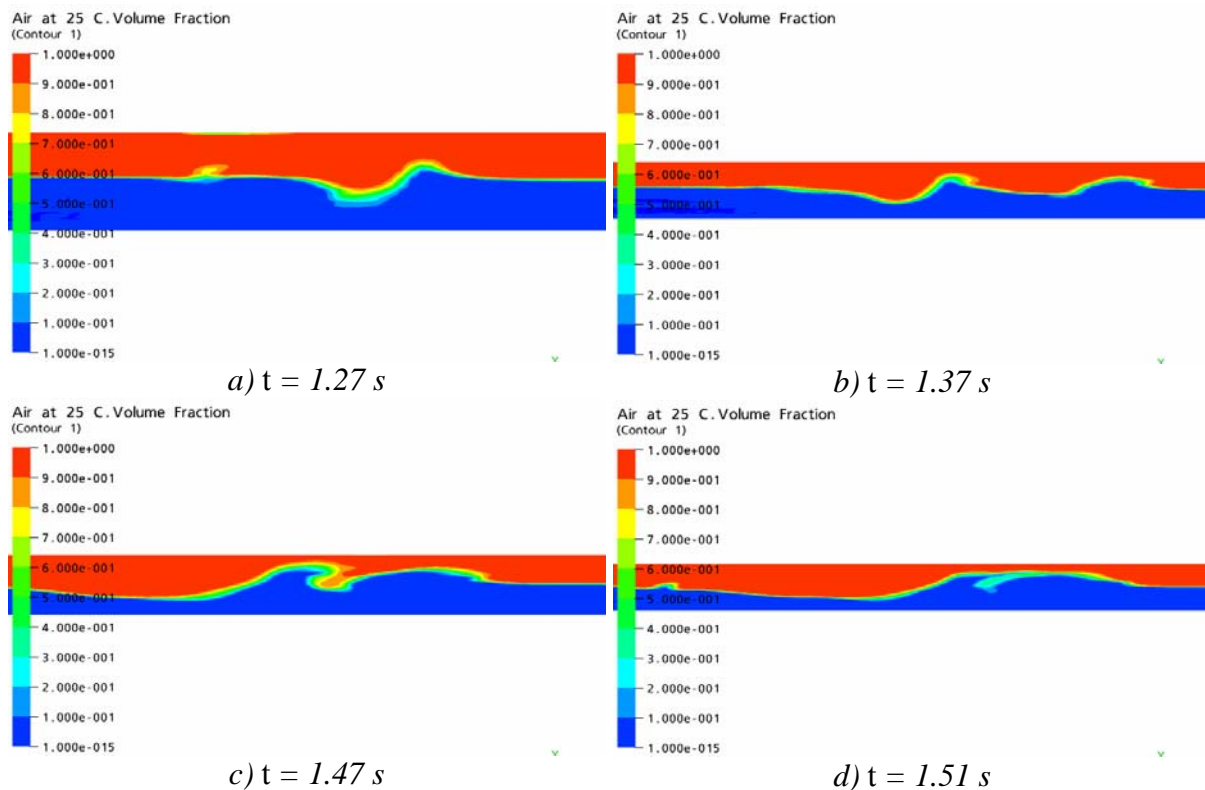


Fig. 7: Details of the slug generation calculated with ANSYS CFX at different simulation time

The needed entrance length for slug generation was defined as the length between the inlet and the location nearest the inlet where a wave closes nearly the entire cross-section. This was observed at about 1.5 m in the experiment and 2.5 m in the calculation.

In contrast to the measurement, the stratified flow after the slug calculated with ANSYS CFX is too smooth which defers the generation of the next slug. Since the slug cleared an important amount of water from the channel, the next slug appears after the channel is slowly filled up again by the transport of liquid from the inlet. This process takes approximately 1.5 s. In the experiment, small waves are generated immediately after the slug and create the next one within 0.3 to maximum 0.7 s. Sources of instabilities are not only the high air velocity but also the pressure surge created by the slugs, particularly when they leave the channel. This effect has not been properly simulated since just the half of the channel was modelled. Therefore, the slug frequency cannot be compared at this stage of the simulation.

5. Summary and conclusions

For the investigation of co-current two-phase flows, the horizontal air/water channel (HAWAC) was built at *Forschungszentrum Dresden-Rossendorf* (FZD). A special inlet device provides well defined as well as variable boundary conditions, which allow very good CFD-code validation possibilities. Optical measurements were performed with a high-speed video camera. The water level history can be extracted from the image sequences by an interface capture method.

A picture sequence recorded during slug flow was compared with the equivalent CFD simulation made with the code *ANSYS CFX*. The two-fluid model was applied with a special free surface treatment. Due to the interfacial momentum transfer, it was possible to generate slugs based on instabilities. The behaviour of slug generation and propagation at the experimental setup was qualitatively reproduced, while deviations in the slug frequency require further work. The creation of small instabilities due to pressure surge or increase of interfacial momentum transfer should be analysed in the future. Furthermore, pressure and velocity measurements should be performed in the HAWAC channel to allow quantitative comparisons.

Due to the success and promising future research activities, the HAWAC was chosen as an OECD Benchmark test facility and as a reference test facility for the German CFD network program.

References

- [1] ANSYS Inc., 2006, ANSYS CFX-10.0 User Manual
- [2] Yegorov, Y. 2004. Contact condensation in stratified steam-water flow, EVOL-ECORA – D 07.

Acknowledgements

This work is carried out in the frame of a current research project funded by the German Federal Ministry of Economics and Labour, project number 150 1265.